L-subshell x-ray cross sections for proton collisions with Pt, Au, and Hg*

James R. Chen
Department of Physics, State University of New York, Geneseo, New York 14454
(Received 12 July 1976)

The L x-ray production cross sections for the $L\alpha_{1,2}$, $L\gamma_{1,5}$, and $L\gamma_{2,3,6}$ transitions in Pt, Au, and Hg have been measured by ionization of the L-subshell electrons with 0.4–2.0-MeV proton bombardment. Individual subshell ionization cross sections, σ_{L_i} (i = 1, 2, or 3), have been extracted from the x-ray yields. Comparisons of the x-ray production and ionization cross-section data have been made with the predictions of the plane-wave Born approximation (PWBA), the PWBA with binding-energy and/or Coulomb-deflection effects, and the constrained binary-encounter approximation (CBEA). The binding-energy and Coulomb-deflection effects partially account for the gross quantitative discrepancies between the PWBA and the data for proton energies less than 1 MeV. Substantial discrepancy still exists, as evidenced by the disagreement between the data for $\sigma_{L_3}/\sigma_{L_2}$ and all the theoretical predictions.

I. INTRODUCTION

The L-shell ionization of atoms due to collisions with incident light ions has been studied by a number of research groups.[1-7] The main features of the L x-ray cross sections for simple projectiles, i.e., protons and helium ions have been established over energies ranging from ~0.2 to ~4 MeV/amu. The agreement between theory and experiment is good for the total production cross sections; the plane-wave Born approximation (PWBA)[8] and the constrained binary-encounter approximation (CBEA)[9] correctly describing the general increase of the total cross-section data with increasing ion energies. Separate contributions of L subshells have been calculated but the experimental data is still sparse. Nevertheless the structure in the L_1-subshell ionization cross section, which is related to the node in the electron wave function in the $2S$ state, has been well established.

With the use of high resolution Si(Li) detectors it has become increasingly feasible to study the finer details of individual subshell ionizations. An earlier paper[10] studied the ratios of the transition rates to a given L_i-subshell (i = 1, 2, or 3) in Ta, Pt, Au, Hg, and Pb. The present paper reports data on the cross sections for individual L_i-subshells in Pt, Au, and Hg by proton collisions (0.4–2.0 MeV) and compares the data with the PWBA and CBEA predictions. In addition comparisons are made between the data and the PWBA including binding energy and Coulomb deflection effects, as prescribed by Brandt and Lapicki.[11] These effects account for the Coulomb deflection of the incident ion through the ion-nuclear interaction and the effect on the L-shell electron binding energy due to the presence of the incident ion inside the L shell during the collision. Recently Gray *et al.*[1] reported discrepancies between the Brandt-Lapicki formulation of the binding energy effect in the PWBA and the x-ray production cross-section data for Sm, Yb, and Pb.

II. EXPERIMENTAL METHOD

As described previously,[10] the protons accelerated by a 2-MeV Van de Graaff were incident on 50–65-μg/cm^2 targets of Pt, Au, and Hg deposited on 20-μg/cm^2 carbon backings and mounted in aluminum frames at 45° to the incident beam. The characteristic x rays were detected in a Si(Li) detector with a resolution of 165 eV full width at half maximum at 5.9 keV. The detector was located directly below the target at 90° to the incident beam and was mounted inside the vacuum system of the target chamber. The absolute efficiency of the detector system was measured using calibrated radioactive sources following established procedures.[12] The absolute efficiency included the intrinsic efficiency of the detector, the fractional solid angle subtended, and the attenuation factor due to the 0.0025-cm Be detector window and a 0.025-cm Mylar cover used to reduce the copious M x rays.

Beam currents were varied between 5 and 50 nA to maintain a count rate of approximately 300 counts/sec. The data were converted to digital format for later analysis on a CDC 6400 computer. The scattered protons were detected by a surface barrier detector mounted at 90° to the incident beam and used to normalize the x-ray cross sections.

III. DATA ANALYSIS

The L x-ray energy spectra can be subdivided into three main groups: the $L\alpha$ group with the weaker Ll and $L\eta$ lines in the tails; the $L\beta$ group; and the $L\gamma$ group.[10] The spectra were analyzed to

give the yields for the $L\alpha_{1,2}$, $L\gamma_{1,5}$, and $L\gamma_{2,3,6}$ transitions. The $L\gamma_6$ transition was included as an unresolved component of the $L\gamma_{2,3,6}$ x-ray line. The $L\beta$ transitions could not be separated into distinct transitions to individual subshells and so were not analyzed.

A. L x-ray production cross sections

The measured x-ray counts were used to obtain the x-ray production cross sections for $L\alpha_{1,2}$, $L\gamma_{1,5}$, and $L\gamma_{2,3,6}$ from

$$\sigma^x_{L_i} = \frac{4\pi(d\sigma/d\Omega)_R(\Delta\Omega)_R}{C_R T_l} \frac{C_{Li}}{\epsilon_{L_i}} . \quad (1)$$

$(d\sigma/d\Omega)_R$ is the Rutherford cross section at a given proton incident energy and scattering angle (90° in these measurements); $(\Delta\Omega)_R$ is the solid angle subtended by the surface barrier detector; C_R is the number of protons detected; T_l is the live time of the system; C_{L_i} is the number of x-ray counts at a given L_i line (with $i = \gamma_{2,3,6}$, $\gamma_{1,5}$, or $\alpha_{1,2}$); and ϵ_{L_i} is the efficiency of the system at the energy of the L_i line, as discussed in Sec. II.

The comparisons to the theoretical predictions of the x-ray production cross sections were made using the relationships discussed in Refs. 3 and 4. Table I lists the values of the parameters used. The subshell fluorescence yields ω_i and the Coster-Kronig transition factors f_{ij} were taken from McGuire.[13] The radiative transition rates τ_i were taken from Scofield.[14] Single hole values for the parameters were used in all cases. The previous works of Gray *et al.*[1] and Pepper *et al.*[15] suggest that multiple ionization is not a major effect to be considered in this work. This assumption must be considered as a possible source of error until more detailed information becomes available.

TABLE I. Radiative and nonradiative parameters used in this work. (See text for references.)

Parameter	Pt	Au	Hg
ω_1	0.104	0.105	0.107
ω_2	0.342	0.357	0.371
ω_3	0.312	0.327	0.341
f_{12}	0.090	0.083	0.078
f_{13}	0.625	0.644	0.654
f_{23}	0.125	0.132	0.128
τ_{L_1}	1.060	1.130	1.220
$\tau_{\gamma_{2,3}}$	0.205	0.220	0.234
τ_{L_2}	1.870	2.000	2.130
$\tau_{\gamma_{1,5}}$	0.310	0.327	0.360
τ_{γ_6}	0.028	0.034	0.041
τ_{L_3}	1.640	1.750	1.860
$\tau_{\alpha_{1,2}}$	1.280	1.360	1.430

B. L_i-subshell ionization cross sections

The $L\gamma_{2,3,6}$ x-ray production cross section contains contributions from both the L_1 subshell (the γ_2 and γ_3 transitions) and the L_2 subshell (the γ_6 transition). This mixture masks the detailed structure of the individual subshell cross sections, in particular that of the L_1 subshell.

To extract the L_1-subshell cross section, the counts in the peak corresponding to the $\gamma_{2,3}$ transition, $C_{L\gamma_{2,3}}$, were separated from $C_{L\gamma_{2,3,6}}$ by using

$$C_{L\gamma_{2,3}} = C_{L\gamma_{2,3,6}} - (\tau_{\gamma_6}/\tau_{\gamma_1})C_{L\gamma_1} , \quad (2)$$

where $\tau_{\gamma_6}/\tau_{\gamma_1}$ is the relative radiative transition probability for the γ_6 to γ_1 transitions.

Ionization cross sections σ_{L_i} to the individual

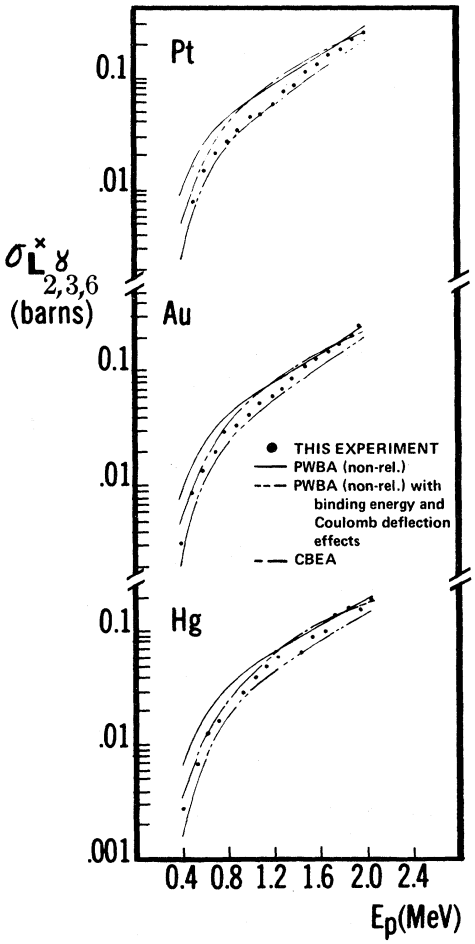

FIG. 1. Experimental x-ray production cross sections for the $L\gamma_{2,3,6}$ transition. The nonrelativistic PWBA calculations are from Ref. 8, the nonrelativistic PWBA with binding energy and Coulomb deflection effects are from Ref. 11, and the CBEA calculations are from Ref. 9.

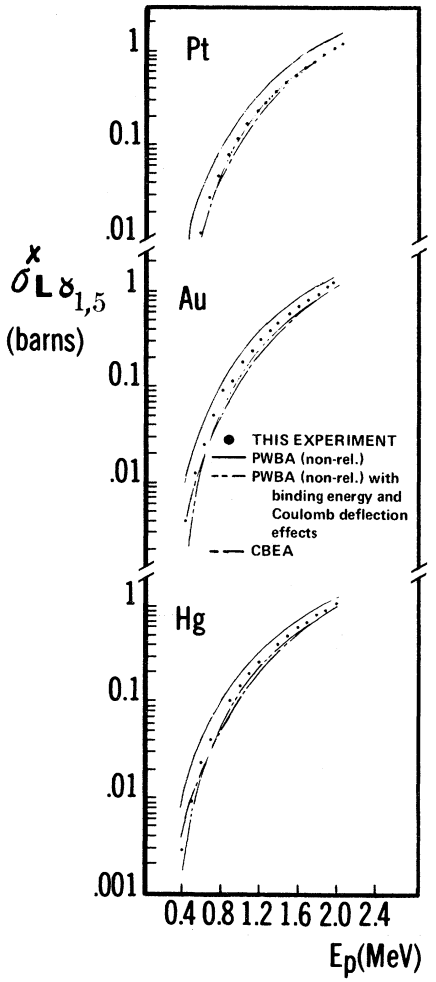

FIG. 2. Experimental x-ray production cross sections for the $L\gamma_{1,5}$ transitions.

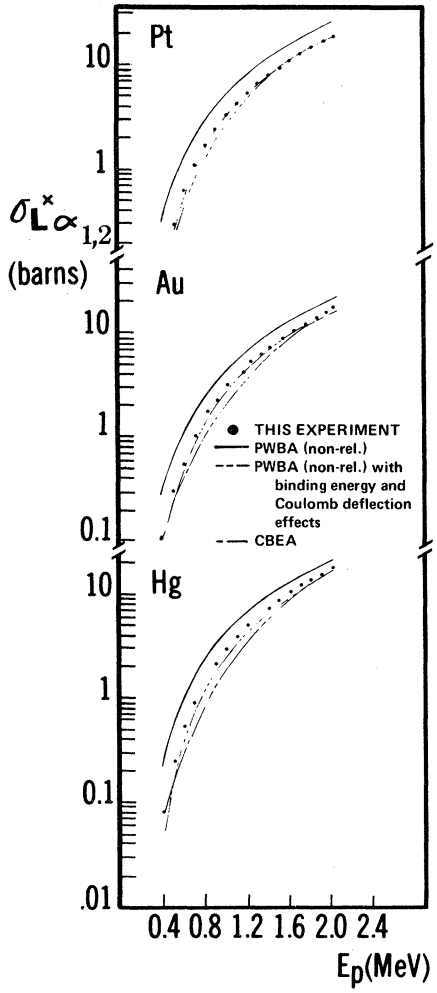

FIG. 3. Experimental x-ray production cross sections for the $L\alpha_{1,2}$ transition.

L_i subshell were obtained using the relationships discussed in Refs. 3 and 4. These were then compared with the predictions of the nonrelativistic PWBA,[8] the nonrelativistic PWBA with binding energy and Coulomb deflection effects,[11] the relativistic PWBA,[16] and the CBEA.[9]

C. Relative and normalization errors

Two main categories of error arise in the treatment of the measured data: (1) the relative uncertainty between data points, which consists of the statistical error (1–2%) associated with C_R, the counts in the charged particle detector, and the statistical error associated with C_{Li}, the counts in the individual x-ray line (<1% for $C_{L\alpha_{1,2}}$; ~2% for $C_{L\gamma_{1,5}}$; ~4% for $C_{L\gamma_{2,3}}$ in Pt and Au and ~8% for $C_{L\gamma_{2,3}}$ in Hg), and (2) the overall normalization uncertainty, which consists of a ~10% uncertainty in the determination of ϵ_{Li}, the efficiency of the detector system, and a ~5% uncertainty associated with determining $(d\sigma/d\Omega)_R(\Delta\Omega)_R$. The contribution from these sources represents a normalization uncertainty of ~11%. The total uncertainties are ~11% for the $L\alpha_{1,2}$ lines, ~12% for the $L\gamma_{1,5}$ lines, and ~12–14% for the $L\gamma_{2,3}$ lines.

IV. DISCUSSION

The experimental values of the x-ray production cross sections $\sigma^x_{Li}(i=\gamma_{2,3,6}, \gamma_{1,5}$, or $\alpha_{1,2})$ obtained from Eq. (1) are plotted in Figs. 1, 2, and 3, respectively, along with the predictions of the nonrelativistic PWBA, the nonrelativistic PWBA with binding energy and Coulomb deflection effects, and the CBEA. The values of the L_i-subshell ionization cross sections σ_{L1}, σ_{L2}, and σ_{L3} are plotted in Figs. 4, 5, and 6, respectively, along with the various theoretical predictions.

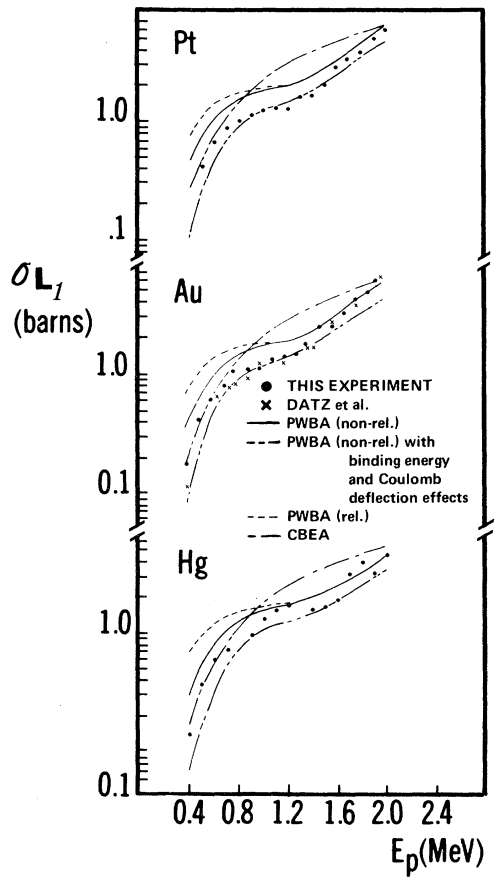

FIG. 4. Values of the ionization cross section to the L_1 subshell σ_{L_1} compared with the various theoretical predictions. The relativistic PWBA are from Ref. 16. The data of Datz *et al.* (Ref. 4) for Au are also shown.

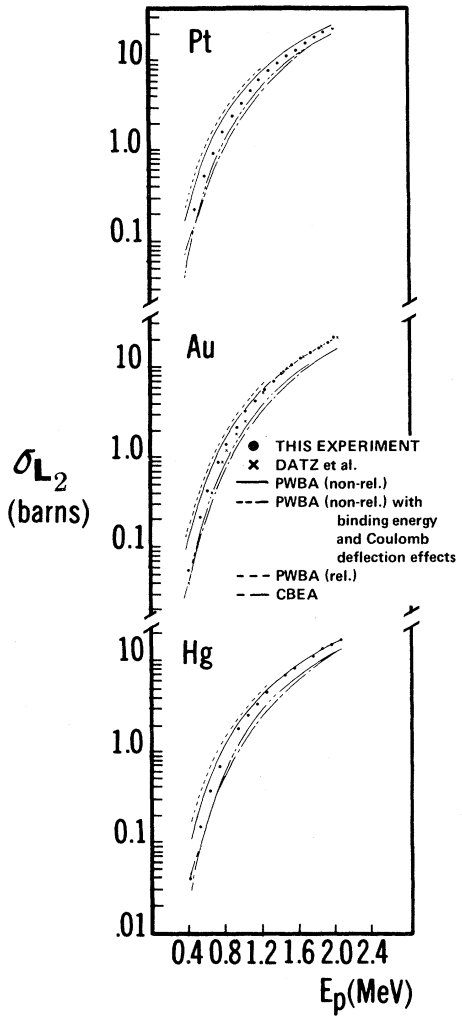

FIG. 5. Values of the ionization cross section to the L_2 subshell σ_{L_2}.

A. L_1-related cross sections

As shown in Fig. 1 the CBEA predictions are not in accord with the experimental data for $\sigma^x_{L\gamma_{2,3,6}}$, which exhibits a slight shoulder in the region $E_p = 0.8-1.2$ MeV. The features of this structure become much clearer in Fig. 4, where the $L\gamma_6$ contamination has been separated from the $L\gamma_{2,3}$ line and only the L_1-subshell ionization cross section is displayed. The plateau in the data is seen to be anticipated by the PWBA model. Similar results have been obtained by Gray *et al.*[1] for Sm, Yb, and Pb, by Tawara *et al.*[2] for Au, Bi, and U, by Chang *et al.*[3] for Ta, Au, and Bi, by Datz *et al.*[4] for Au, and by Madison *et al.*[5] for Pb and Bi.

Although the nonrelativistic PWBA follows the general shape of σ_{L_1} and agrees in magnitude with the data within the experimental errors above $E_p = 1.5$ MeV, for lower incident proton energies the nonrelativistic PWBA predictions are on the average a factor of 1.6 above the data for Pt, Au, and Hg. Between 0.4–1.0 MeV the relativistic PWBA is a factor of 2 greater than the data.

These discrepancies indicate the inadequacy of the PWBA at low proton velocities for the high Z targets used. The results of including the binding energy and Coulomb deflection effects in the PWBA, as prescribed by Brandt and Lapicki,[11] is to decrease the cross-section predictions. As Fig. 4 depicts, with the inclusion of these effects in the PWBA, the gross disparities between theory and data are removed, but the theory tends to overcorrect in predicting the σ_{L_1} cross sections. These results are closely correlated to similar results obtained by Brandt and Lapicki[11] for the Au L_1-subshell data of Datz *et al.*,[4] and by Gray *et al.*[1] for data on Sm, Yb, and Pb L_1 subshells.

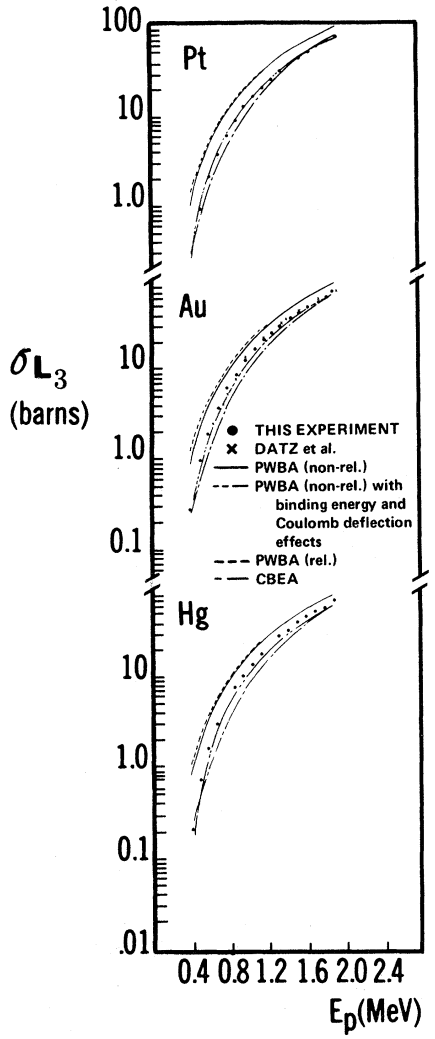

FIG. 6. Values of the ionization cross section to the L_3 subshell σ_{L_3}.

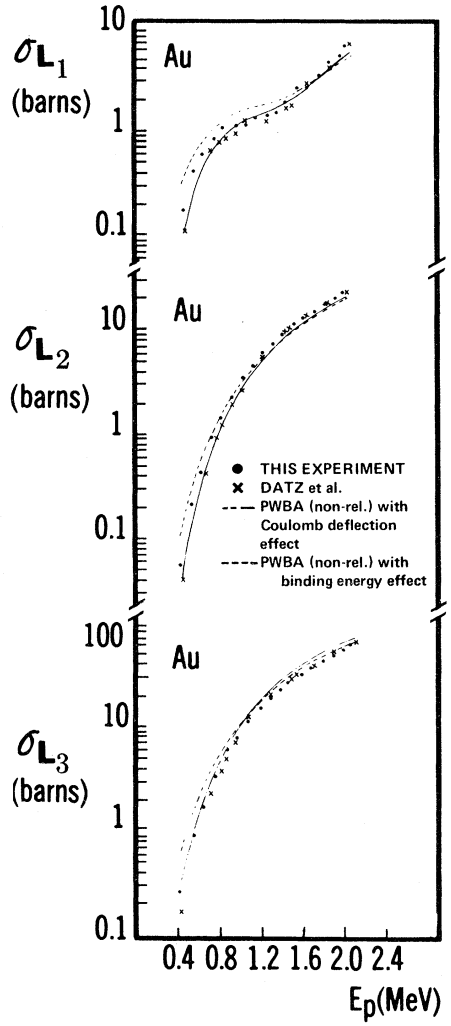

FIG. 7. Values of the ionization cross section to the L_1, L_2, and L_3 subshells in Au compared to the nonrelativistic PWBA with the Coulomb deflection effect and the binding energy effect included separately, as obtained from Ref. 11. The data of Datz *et al.* (Ref. 4) are also shown.

B. L_2-related cross sections

As observed in Figs. 2 and 5, $\sigma^x_{L\gamma_{1,5}}$ and σ_{L_2} show the same general trends as the $\sigma^x_{L\gamma_{2,3,6}}$ and σ_{L_1} cross sections. The PWBA predictions generally agree with the data except for $E_p < 1.2$ MeV, while the nonrelativistic PWBA with binding energy and Coulomb deflection effects overcorrects in lowering the theoretical predictions.

C. L_3-related cross sections

Figures 3 and 6 show the comparison of the data for $\sigma^x_{L\alpha_{1,2}}$ and σ_{L_3} with the various theoretical predictions. For all three elements the agreement between the experimental data and the nonrelativistic PWBA with binding energy and Coulomb deflection effects is striking. This result is in agreement with similar results obtained by Gray *et al.* for Sm, Yb, and Pb and by Brandt and Lapicki for the Au data of Datz *et al.*

Figure 7 shows the L_i-subshell ionization cross sections for Au along with the predictions of the PWBA with the binding energy and the Coulomb deflection effects included separately. For σ_{L_1} above $E_p = 1.4$ MeV both effects overcorrect, while below 1.4 MeV the binding energy effect is not sufficient to bring the PWBA in line with the data. A similar result holds for σ_{L_2}. Both effects are needed to bring the PWBA in agreement with the σ_{L_3} data. Figure 8 shows the data for the ionization cross section ratio $\sigma_{L_1}/\sigma_{L_2}$, in Pt, Au, and

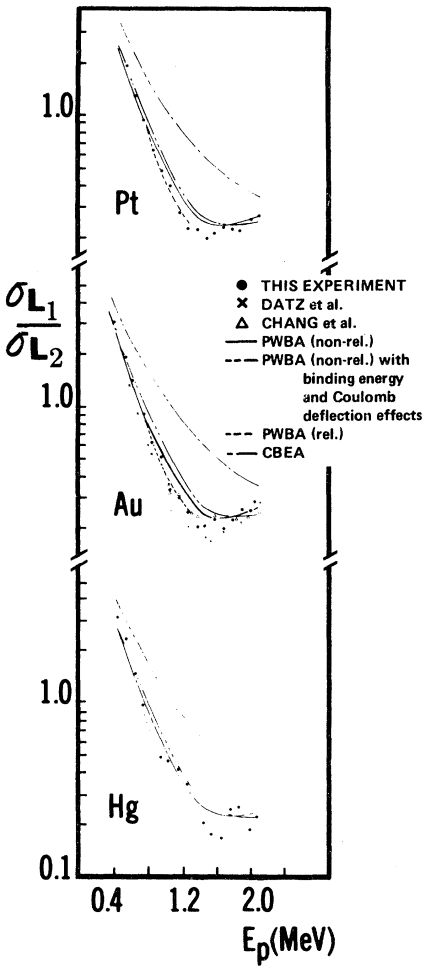

FIG. 8. Values of the ionization cross section ratio, $\sigma_{L_1}/\sigma_{L_2}$, compared with the various theoretical predictions. The data of Datz *et al.* (Ref. 4) and Chang *et al.* (Ref. 3) for Au are also shown.

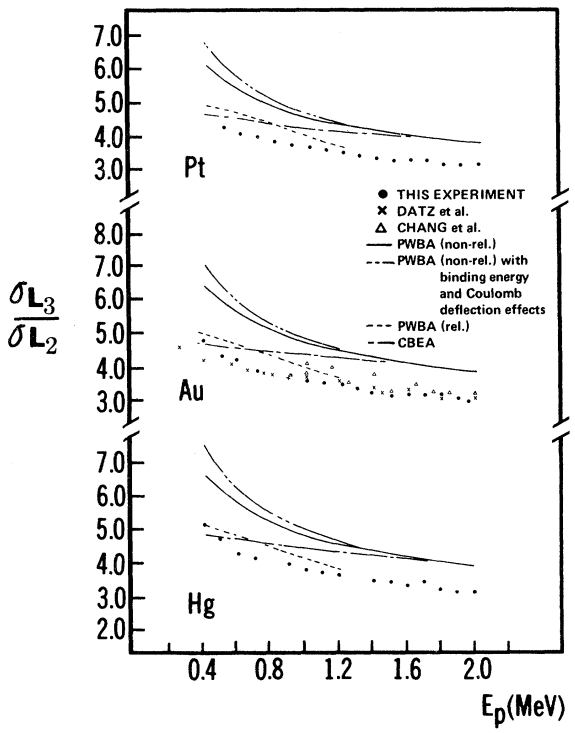

FIG. 9. Values of the ionization cross section ratio $\sigma_{L_3}/\sigma_{L_2}$ compared with the various theoretical predictions. The data of Datz *et al.* (Ref. 4) and Chang *et al.* (Ref. 3) for Au are also shown.

Hg. The accuracy of the data is not sufficient to distinguish between the positions of the minimum predicted by the nonrelativistic PWBA with and without the binding energy and Coulomb deflection effects.

Gray *et al.*[1] have pointed out that there are problems with the binding energy correction as utilized in the Brandt-Lapicki calculations; it causes a shift in the structure associated with the 2*S* ionization cross section. They found that the predicted shift is pronounced for He and Li incident ions, which is not supported by the experimental data. For H bombardment, they found the shift to be minimal; the curves depicted in Fig. 8 support this conclusion.

That further studies are needed can be seen in Fig. 9. There is evident disagreement between the $\sigma_{L_3}/\sigma_{L_2}$ data and all the theoretical predictions. The nonrelativistic PWBA follows the shape of the data but differ in overall normalization by a factor of 0.75. The ratio $\sigma_{L_3}/\sigma_{L_2}$ is somewhat better fitted by the relativistic PWBA.

V. CONCLUSIONS

The measurements of the L x-ray yields in Pt, Au, and Hg have been used to extract experimental x-ray production cross sections $\sigma^x_{L_i}$ ($i=\gamma_{2,3,6}$, $\gamma_{1,5}$, or $\alpha_{1,2}$) and ionization cross sections to the individual L_i subshell, σ_{L_i} ($i=1, 2$, or 3).

The PWBA calculations predict the observed plateau in σ_{L_1}, while the CBEA does not. Above $E_p=1$ MeV the PWBA predictions are in agreement with the data, but at lower energies substantial discrepancies exist. For σ_{L_2} and σ_{L_3} both the nonrelativistic and relativistic PWBA predictions generally lie above the data. This is in agreement with the work of other research groups.[1-7]

The above discrepancies are partially accounted for when the effects of increased binding energy of the L-shell electrons due to the presence of the bombarding proton inside the L shell during the collision and the Coulomb deflection of the bombarding proton by the target nucleus are included in the nonrelativistic PWBA, as prescribed by

Brandt and Lapicki. With the inclusion of these effects the agreement with the σ_{L_3} ionization cross-section data is excellent; however, the theory overcorrects in predicting the σ_{L_1} and σ_{L_2} cross-sections.

When the binding energy and Coulomb deflection effects are included in the nonrelativistic PWBA separately, it is found that both effects are needed to bring the PWBA in agreement with the σ_{L_3} data, while both effects overcorrect in predicting σ_{L_1} and σ_{L_2} above $E_p \simeq 1.4$ MeV.

Discrepancies still exist as evidenced by the disagreement between the data for $\sigma_{L_3}/\sigma_{L_2}$ and all the theoretical predictions.

ACKNOWLEDGMENTS

The author wishes to thank Professor W. Brandt, Professor T. J. Gray, Professor K. Kinsey, Professor G. Lapicki, and Professor P. V. Rao for having read and commented on the manuscript.

---

*Work supported in part by grants from the Research Foundation of SUNY.

[1]T. J. Gray, G. M. Light, R. K. Gardner, and F. D. McDaniel, Phys. Rev. A 12, 2393 (1975).

[2]H. Tawara, K. Ishii, S. Morita, H. Kaji, and T. Shiokawa, Phys. Rev. A 11, 1560 (1975).

[3]C. N. Chang, J. F. Morgan, and S. L. Blatt, Phys. Rev. A 11, 607 (1975); Phys. Lett. 49A, 365 (1974).

[4]S. Datz, J. L. Duggan, L. C. Feldman, E. Laegsgaard, and J. V. Andersen, Phys. Rev. A 9, 192 (1974).

[5]D. H. Madison, A. B. Baskin, C. E. Busch, and S. M. Shafroth, Phys. Rev. A 9, 675 (1974).

[6]S. M. Shafroth, G. A. Bissinger, and A. W. Waltner, Phys. Rev. A 7, 566 (1973).

[7]C. E. Busch, A. B. Baskin, P. H. Nettles, S. M. Shafroth, and A. W. Waltner, Phys. Rev. A 7, 1601 (1973).

[8]B.-H. Choi, E. Merzbacher, and G. S. Khandelwal, At. Data 5, 291 (1973).

[9]J. S. Hansen, Phys. Rev. A 8, 822 (1973).

[10]J. R. Chen, J. D. Reber, D. J. Ellis, and T. E. Miller, Phys. Rev. A 13, 941 (1976); Bull. Am. Phys. Soc. 21, 33 (1976).

[11]W. Brandt and G. Lapicki, Phys. Rev. A 10, 474 (1974).

[12]J. S. Hansen, J. C. McGeorge, D. Nix, W. D. Schmitt-Ott, I. Unus, and R. W. Fink, Nucl. Instrum. Methods 106, 365 (1973); R. J. Gehrke and R. A. Lokken, Nucl. Instrum. Methods 97, 219 (1971); and L. B. Magnusson, Phys. Rev. 107, 161 (1957).

[13]E. J. McGuire, Phys. Rev. A 3, 587 (1971).

[14]J. H. Scofield, Phys. Rev. A 10, 1507 (1974); 12, 345(E) (1975).

[15]G. H. Pepper, R. D. Lear, T. J. Gray, R. P. Chaturvedi, and C. F. Moore, Phys. Rev. A 12, 1237 (1975).

[16]B.-H. Choi, Phys. Rev. A 4, 1002 (1971); H. Hönl, Z. Phys. 84, 1 (1933).